

Chemical Science

Accepted Manuscript



This is an *Accepted Manuscript*, which has been through the Royal Society of Chemistry peer review process and has been accepted for publication.

Accepted Manuscripts are published online shortly after acceptance, before technical editing, formatting and proof reading. Using this free service, authors can make their results available to the community, in citable form, before we publish the edited article. We will replace this *Accepted Manuscript* with the edited and formatted *Advance Article* as soon as it is available.

You can find more information about *Accepted Manuscripts* in the [Information for Authors](#).

Please note that technical editing may introduce minor changes to the text and/or graphics, which may alter content. The journal's standard [Terms & Conditions](#) and the [Ethical guidelines](#) still apply. In no event shall the Royal Society of Chemistry be held responsible for any errors or omissions in this *Accepted Manuscript* or any consequences arising from the use of any information it contains.

EDGE ARTICLE

Ratiometric Delivery of Cisplatin and Doxorubicin using Tumour-Targeting Carbon-Nanotubes Entrapping Platinum(IV) Prodrugs

Cite this: DOI: 10.1039/x0xx00000x

Chee Fei Chin,^a Siew Qi Yap,^a Jian Li,^b Giorgia Pastorin^{*b,c,d} and Wee Han Ang^{*a}Received 00th January 2012,
Accepted 00th January 2012

DOI: 10.1039/x0xx00000x

www.rsc.org/chemicalscience

Combination therapy is an effective strategy to enhance the efficacy of single-agent chemotherapy and delay onset of chemoresistance. However, differences in the pharmacokinetic profiles of the drug constituents can complicate the implementation of combination regimens in a clinical setting. Nanomaterials can overcome these limitations by offering a unified platform for targeted and synchronous delivery of multiple drugs, although exact ratiometric loading cannot be assured using conventional encapsulation techniques. An approach was conceived with the goal of delivering exact stoichiometric proportions of cisplatin and doxorubicin against endometrial adenocarcinoma using tumour-targeting multiwalled carbon nanotubes entrapping an inert Pt(IV) prodrug. Activation of the Pt(IV) prodrug after cell entry synchronously releases molar equivalents of hydrophilic cisplatin and doxorubicin from the hydrophobic confines thereby achieving ratiometric delivery of these mechanistically-complementary drug entities.

Introduction

Cancer drug resistance, the diminishing efficacy of specific chemotherapeutic agents towards their targets, poses one of the most serious challenges in modern cancer medicine.¹ The underlying mechanisms upon which the resistance phenomena emerge is complex and differ across the spectrum of different cancer phenotypes.² Yet they point towards the interconnectivity and complexity of the various molecular pathways in cancer biology, giving rise to multiple redundancies by which these aberrant cells can survive and proliferate.³ One strategy that is widely employed to combat chemoresistance is combination therapy. By administering a cocktail of different anticancer drugs working against different targets, combination therapy aims to deter the development of drug resistance by defeating cellular survival pathways in a

multi-pronged assault and overcoming defence mechanisms through therapeutic synergism.⁴

There are unique challenges involved in delivering drug combinations in a clinical setting.⁵ Drugs with different pharmacokinetic properties are differentially distributed which directly affect their concentrations at the intended target. Consequently, it is difficult to control the constituent drug levels of the combination regimen as well as coordinate their delivery to the site of action. These factors explain why remarkable *in vitro* efficacies against cancer cell models does not necessarily translate into effective clinical formulations. One strategy that has been garnering much interest in recent years is the use of nanoscale carriers to deliver drug combinations that are covalently or non-covalently encapsulated.⁶ These vehicles enable the synchronous transport of the different drugs to their site of action as well as provide a platform upon which targeted delivery could be designed. By unifying these two properties, nanocarriers could in principle deliver combination regimens with highly controlled drug proportions and loading.⁵ However, exact ratiometric delivery of different drugs using nanomaterials remains elusive because current encapsulation techniques invariably produce nanocomposites that contain a statistical distribution of encapsulated drugs. This non-uniformity is further amplified when two or more drugs are being combined, adding to greater variances.⁷

^aDepartment of Chemistry, National University of Singapore, Singapore 117543. Tel: +65 6516 5131; E-mail: chmawh@nus.edu.sg

^bDepartment of Pharmacy, National University of Singapore, Singapore 117543. Tel: +65 6516 1876; E-mail: phapg@nus.edu.sg

^cNUS Graduate School for Integrative Sciences and Engineering, Centre for Life Sciences (CeLS), Singapore 117456, Singapore

^dNanoCore, Faculty of Engineering, National University of Singapore, Singapore 117576, Singapore

† Electronic Supplementary Information (ESI) available: Synthesis and characterization of Pt complexes, preparation of Pt-containing MWCNTs, TEM images of MWCNTs, and *in vitro* experiments. See DOI: 10.1039/b000000x/

One of the most important and effective anticancer drug used in the clinic is cisplatin (cDDP, Fig. 1).⁸ Together with bleomycin and etoposide (Chart S1), it forms the first-line chemotherapy against testicular carcinoma.⁹ It is also being investigated extensively with other FDA-approved drugs such as gemcitabine,¹⁰ etoposide,¹¹ and docetaxel/fluorouracil¹² against a spectrum of malignancies (Chart S1). cDDP acts through covalent binding with DNA purine bases,¹³ and the platinated DNA adducts formed strongly inhibit cellular processes such as transcription and replication, ultimately leading to apoptosis.¹⁴ However, cDDP is limited by high toxicity and severe side-effects as well as incidences of Pt-associated drug resistance.¹⁵

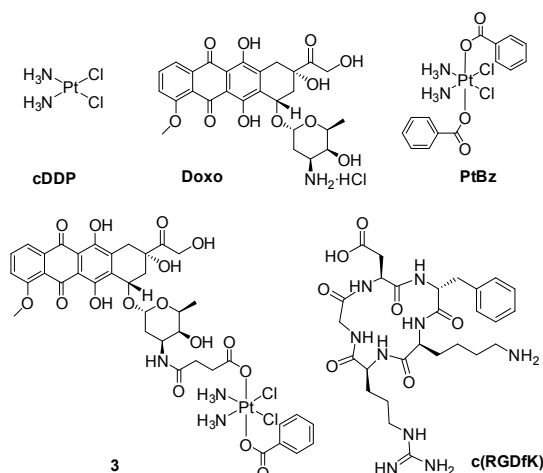


Fig. 1 Molecular structures of cisplatin (cDDP), doxorubicin (doxo) and compounds investigated in this report

To overcome these limitations, cDDP has been investigated in combination with anthracycline-based topoisomerase II (TOP2)-inhibitors against human lung cancer cell lines and found to greatly enhance the overall activity.¹⁶ TOP2 inhibitors intercalate duplex DNA and the resultant DNA-adducts formed inhibit the progression of TOP2 in the process of DNA remodelling. Because this pathway is independent of DNA alkylation damage induced by cDDP, together they can overwhelm the cellular repair mechanisms.¹⁷ A recent Phase III clinical trials found that overall therapeutic efficacy was improved when cDDP was co-administered with TOP2 inhibitor doxorubicin (Doxo, Fig. 1) against endometrial adenocarcinoma.¹⁸ In comparison to single agent Doxo, the combination chemotherapy of Doxo with cDDP resulted in higher but acceptable toxicity, and a significantly higher response rate with modest survival benefit was achieved. Doxo:cDDP combination regimens have also been evaluated in other clinical trials against several other malignancies with positive results. In these therapies, patients were dosed with Doxo:cDDP ratios of between ca. 0.9 to 3.0 molar equivalents cDDP with respect to Doxo.¹⁸⁻¹⁹

The entrapment of cDDP and Doxo in nanoscale carriers can reduce toxicities by achieving targeted localization in tumours and preventing premature release of drugs.⁶ Nguyen *et*

al. demonstrated this strategy through co-delivery of Doxo and the $[cis-Pt(NH_3)_2]^{2+}$ pharmacophore using a lipid-templated polymer-caged nanobin platform.²⁰ The release mechanisms of the two drug entities were different: the $[cis-Pt(NH_3)_2]^{2+}$ pharmacophore was liberated from the polymer support via aqutation while Doxo was released upon protonation. Significantly lower drug dosage was required when the drugs were encapsulated in the nanocarrier against several cancer cell lines than when they were administered together or independently. In a related work, Lippard *et al.* demonstrated that the co-encapsulation of paclitaxel with a polymer-bound Pt(IV) prodrug of cisplatin formed self-assembled biocompatible nanoparticles capable of dual delivery of the two drugs.²¹ Accurate control over the drug composition was achieved and the drug nanocomposite demonstrated significantly improved activities against prostate cancer cells *in vitro* and *in vivo*.

In order to realise the goal of exact ratiometric drug delivery, we conceived a new approach using a tumour-targeting multi-walled carbon nanotube (MWCNT)-based delivery vehicle. The strategy is centred on the intracellular reduction of an inert Pt(IV) prodrug, that is stably entrapped within the MWCNT, which simultaneously releases cDDP and Doxo (Fig. 2). Previously, CNTs have been widely studied *in vitro* and *in vivo* as a means of delivering Doxo.²² To achieve tumour-targeting, the MWCNT carrier was surface-functionalized with an integrin-targeting cyclic peptide c(RGDfK) (Fig. 1). As a proof of concept, we report the formulation of this MWCNT-Pt(IV) prodrug nanoconjugate capable of synchronous ratiometric delivery of two mechanistically complementary drugs and demonstrate its efficacy against ovarian and endometrial cancer cells.

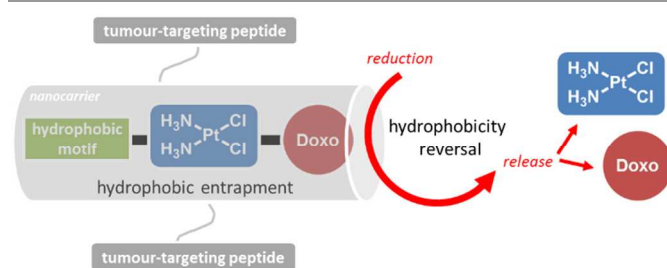


Fig. 2 Concept of ratiometric dual-drug delivery via hydrophobic entrapment using MWCNTs as a nanocarrier

Results and discussion

In order to simultaneously delivering both drug entities in exact ratiometric proportions, we designed a Pt(IV) prodrug **3** (Fig. 1) based on the cDDP template containing Doxo at one of its axial ligand position. In order to tune its lipophilicity, a hydrophobic benzoate motif was added to the other axial position. We and others have previously shown these asymmetric Pt(IV) prodrugs to be highly versatile platforms as they can be reduced into cDDP while their axial ligand positions offer opportunity for functionalization without

affecting the Pt(II) pharmacophore.²³ These Pt(IV) complexes are substitutionally inert and do not undergo rapid aquation to form reactive aqua species.²⁴ By tuning its ligand properties, we previously demonstrated that Pt(IV) prodrug PtBz (Fig. 1) can be stably entrapped within the MWCNT cavities *via* strong hydrophobic-hydrophobic interactions.²⁵ Upon cell entry, chemical reduction by intracellular reductants converted PtBz to hydrophilic cDDP and was consequently discharged from the MWCNT carrier. We considered that being hydrophilic, Doxo would be incompatible with MWCNT entrapment. Therefore by engineering Doxo as hydrophobic Pt(IV) prodrug **3**, stable MWCNT entrapment could be ensured.

Asymmetric Pt(IV) complex **1** was synthesized according to previously reported procedure and treated with excess succinic anhydride in DMF to yield **2** bearing a carboxylic functional group.²⁶ Complex **2** was coupled to Doxo in DMF with *O*-benzotriazole-1-yl *N,N,N',N'*-tetramethyluronium hexafluoro-phosphate (HBTU) as a coupling reagent under room conditions. The product **3** was recovered from the crude reaction mixture *via* lyophilisation and repeated washing using water, acetone and diethyl ether. Previous attempts to synthesize **3** using *N,N'*-dicyclohexylcarbodiimide and ethyl(dimethylaminopropyl)carbodiimide as coupling reagents resulted in poor yields. Complex **2** and **3** were characterized using ESI-MS and ¹H NMR spectroscopy. The parent molecular ions [M-H]⁻ were readily observed using ESI-MS. Fragmentation analysis for **2** resulted in the loss of NH₃, HCl, and carboxylate ligands while fragmentation analysis for **3** resulted in the loss of the Doxo ligand, consistent with the proposed structures. Characteristic resonances could be observed at ca. 6.6 ppm in ¹H NMR, assigned to the ammine ligands, were consistent with other reported Pt(IV) bis-carboxylates.²⁶⁻²⁷ The formation of **3** was also indicated by the disappearance of the -COOH proton at 12.0 ppm. In addition, the integral value in ¹H NMR showed that there is only one unit of Doxo with respect to the ammine ligands.

Ultrapure (≥98%) MWCNTs with a diameter of 30-40 nm and a length of up to a few μm were used given their higher internal loading capacity compared to single-walled CNTs. These pristine MWCNTs were oxidized and purified in accordance with a reported procedure to yield MWCNT_{oxidized} (Fig. 3b),²⁸ and coupled with bifunctional 2,2'-(ethylenedioxy)diethylamine (TEG) using EDC/DIPEA to obtain amine-terminated MWCNTs (MWCNT_{TEG}). Quantitative Kaiser Test was performed to determine the degree of amino-functionalization on MWCNT_{TEG} and ascertained to be 680 μmol of -NH₂ groups per gram of MWCNTs. The purified and dried MWCNTs were subsequently treated with excess of succinic anhydride in DMSO at r.t. for 3 d to form carboxylic acid-terminated MWCNTs (MWCNT_{TEG-COOH}). A negative Kaiser Test indicated that the amine groups on the MWCNTs were fully converted to carboxylic acid functional groups.

To achieve tumour-targeting, c(RGDfK) peptide was conjugated to the MWCNT platform (Fig. 1). These peptides recognize multiple ligands of α_v integrin family,²⁹ and exhibit

high affinity to α_vβ₃ and α_vβ₅ integrin receptors which are overexpressed in tumor angiogenic endothelial cells.³⁰ Hence, they are particularly relevant for endometrial adenocarcinomas since vascular endothelial growth factor, which is correlated with angiogenesis, is the major stimulus for endothelial cell proliferation in this cancer phenotype.³¹ MWCNT_{TEG-COOH} coupled to c(RGDfK) peptide using HBTU/Net₃ to obtain MWCNT_{c(RGDfK)} (Fig. 3b). The formation of MWCNT_{c(RGDfK)} was accompanied by a mass change of more than 50%. For hydrophobic entrapment, purified MWCNT_{c(RGDfK)} was suspended with **3** in solvent and agitated for 3 d in accordance with a previously reported procedure.²⁵ We utilized water or CHCl₃ as the drug entrapment solvent for nanoextraction since they poorly solubilize both **3** and MWCNT_{c(RGDfK)} and would enhance their hydrophobic-hydrophobic interactions. The entrapped product [**3**-MWCNT_{c(RGDfK)}] was filtered and washed extensively with a washing solvent mixture comprising water:CHCl₃:MeOH (1:2:2.5 v/v). This washing step was essential to remove unbound **3** on the external MWCNT surface without displacing those entrapped within the core. Being intensely red in colour, complete removal of unbound **3** was indicated by clear washings and restoration of the MWCNTs as a black residue.

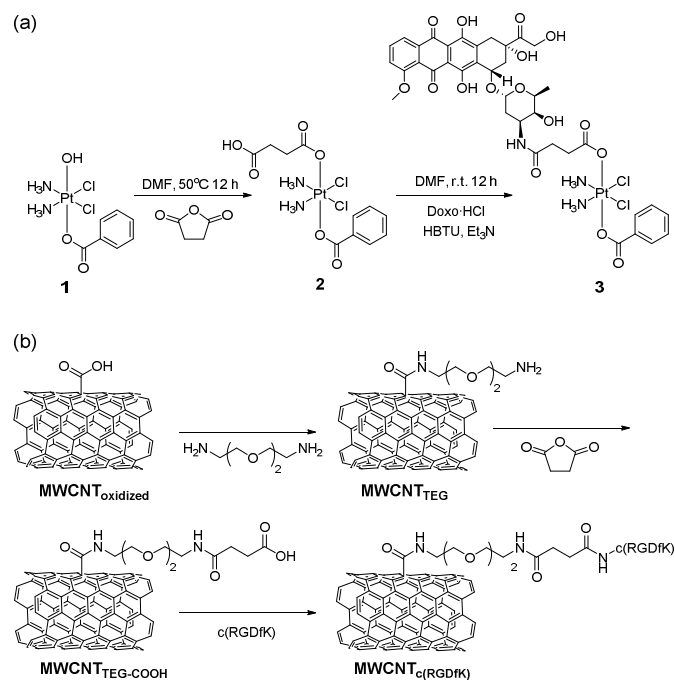


Fig. 3 Synthetic scheme for (a) preparation of **3** and (b) surface functionalization of MWCNT

Pt content in [**3**-MWCNT_{c(RGDfK)}] was determined using ICP-OES on samples that were incinerated at 1000°C and their residues reconstituted in 2% HNO₃. Based on the Pt levels quantitated, the entrapment levels within MWCNT_{c(RGDfK)} using CHCl₃ and water as solvent systems were ascertained to be 17.0 ± 1.0% and 24.5 ± 0.8% w/w of **3**, respectively. In previous

reports, entrapment efficiencies of cDDP and PtBz in $\text{MWCNT}_{\text{oxidized}}$ were higher at $62.1 \pm 2.0\%$ w/w and $51.7 \pm 2.0\%$ w/w, respectively.²⁵ The lower $[\mathbf{3} \cdot \text{MWCNT}_{\text{c(RGDfK)}}]$ loading was presumably due to its increased steric encumbrance resulting in poorer mobility within the CNT cavity.

To achieve targeted delivery, drug payload should only be released at the site of its intended target. To demonstrate that $[\mathbf{3} \cdot \text{MWCNT}_{\text{c(RGDfK)}}]$ can function effectively as a delivery platform for controlled intracellular release of its payload, we investigated the stability of **3** entrapped within $\text{MWCNT}_{\text{TEG}}$ under reducing and non-reducing aqueous conditions. For comparison, we prepared entrapped Doxo and monitored its release from $\text{MWCNT}_{\text{TEG}}$ using UV-vis spectroscopy (λ_{550}). Under aqueous conditions, Doxo release from $\text{MWCNT}_{\text{TEG}}$ was rapid with >50% of the payload released within 10 h (Fig. 4). Complete drug release was achieved after 4 d. Entrapped **3**, on the other hand, was stable within $\text{MWCNT}_{\text{amine}}$ and uncontrolled release of Doxo into the surrounding environment was not observed. Only after 4 d was ca. 10% Doxo w/w non-specifically released into the media. However, in the presence of a reductant, i.e. 3 mM ascorbic acid, release of Doxo was observed culminating with complete release after 4 d. Transmission electron microscopy images showed that the MWCNTs remained structurally intact after the contents have been released (Fig. S4). In this manner, controlled release of the hydrophobically entrapped drug payload was achieved using reduction of the Pt(IV) scaffold.

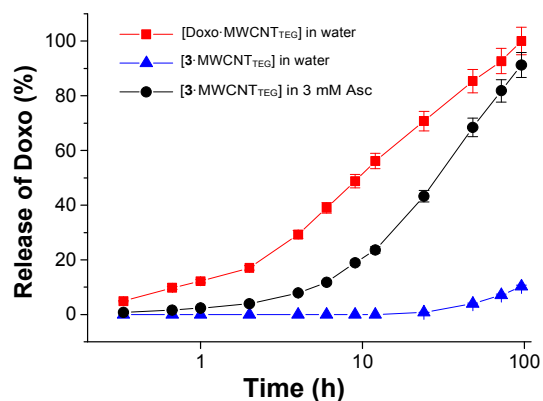


Fig. 4 Release of Doxo from $\text{MWCNT}_{\text{TEG}}$ monitored using UV-vis spectroscopy (λ_{550})

Chemical reduction by ascorbic acid reduced the Pt(IV) prodrug to Pt(II) while liberating its axial ligands, namely benzoate and doxo-succinate. Because these components are hydrophilic, they cannot be stably entrapped within MWCNTs and are extruded. We have earlier shown that upon reduction, Pt(IV) prodrug (PtBz, Fig. 1) entrapped in $\text{MWCNT}_{\text{oxidized}}$ released Pt(II) species into the media which bind deoxyguanosine monophosphate (dGMP). Otherwise, entrapped PtBz did not react with dGMP implying that they are able to exert their cytotoxic effects only upon release from the carrier. One significant difference with earlier findings is the slower rate of release of the contents. We attribute this to

slower kinetics to increased steric encumbrance at the cavity entrances due to surface functionalization on $\text{MWCNT}_{\text{c(RGDfK)}}$.

The efficacy of the new constructs on the growth inhibition of Ishikawa endometrial adenocarcinoma as well as A2780 and A2780/Cis human ovarian carcinoma cells was investigated (Table 1). Adherent cells were exposed to varying concentrations of test compound in serum-free medium for 6 h before replacing with complete media and a further incubation period of 66 h. The viability of the remaining cells was determined using the MTT assay and the data was presented as % survival against non-treated controls. The concentration required to inhibit 50% of cell viability (IC_{50}) was interpolated from the plots and tabulated (Table 1). To further mitigate the effects of contamination, Pt concentration of the stock solutions were determined using ICP-OES and the IC_{50} values were adjusted to actual Pt concentration values for entries 1, 3, 4 and 6.

Table 1 IC_{50} values (μM) against cancer cell lines^a

Entry	Test compound ^b	A2780	A2780/Cis	Ishikawa
1	cDDP	1.71 ± 0.42	13.11 ± 1.99	11.10 ± 0.80
2	Doxo	0.92 ± 0.48	0.89 ± 0.15	2.96 ± 0.15
3	cDDP + Doxo (1:1)	0.84 ± 0.02	1.17 ± 0.11	2.35 ± 0.25
4	3	3.29 ± 0.72	4.82 ± 0.28	6.76 ± 0.44
5	$[\text{MWCNT}_{\text{c(RGDfK)}}]^c$	N.D	N.D	N.D
6	$[\mathbf{3} \cdot \text{MWCNT}_{\text{c(RGDfK)}}]$	0.76 ± 0.17	0.90 ± 0.30	0.95 ± 0.06

^aConcentration required to inhibit 50% of the cell growth with respect to control groups, measured by MTT assay after 72 h exposure. ^bData obtained are based on the average of at least three independent experiments with the corresponding standard deviations. ^cEmpty $\text{MWCNT}_{\text{c(RGDfK)}}$ were tested and inhibition of cell viability was not observed at >50 $\mu\text{g/mL}$ which exceeded the concentrations tested for entry 6.

Cisplatin exerts its cytotoxic effects through DNA alkylation which yield primarily intrastrand platinated adducts on purine bases. Such adducts have previously been shown to be strongly inhibit RNA pol by impeding its passage during transcription.³² Stalling of the transcription complex at the platinated site triggers the nuclear excision repair pathway and excision of aberrant adduct from the DNA strand.³³ On the other hand, Doxo, a DNA intercalator, prevents the progression of TOP2 during DNA remodelling leading to stalling of TOP2 at the adduct site.³⁴ Due to these complimentary mechanisms acting on the same biological target, we postulated that a combination of these drugs could lead to synergistic enhancement of cytotoxicity. As anticipated, Doxo exerted a strong cytotoxic effect against both A2780 and A2780/Cis indicating that its mode of action was independent of the cDDP resistance pathway. We further noted that a 1:1 combination of cDDP and Doxo was additive which could be due to differential uptakes of the two drugs. With that aim, we developed a new MWCNT construct $[\mathbf{3} \cdot \text{MWCNT}_{\text{c(RGDfK)}}]$ containing a Pt(IV) prodrug that is capable of delivering cDDP + Doxo in stoichiometric-equivalent portions. $[\mathbf{3} \cdot \text{MWCNT}_{\text{c(RGDfK)}}]$ was more efficacious against the tested cell lines compared to

cDDP, Doxo or a physical mixture of cDDP + Doxo (1:1). In keeping with Doxo, [3·MWCNT_{c(RGDfK)}] was also able to overcome A2780/Cis. Strikingly, against target Ishikawa endometrial adenocarcinoma cells, [3·MWCNT_{c(RGDfK)}] was ca. 2-fold more cytotoxic than either Doxo or cDDP + Doxo 1:1 combination and 11-fold more than cDDP alone.

We compared IC₅₀ values of [3·MWCNT_{c(RGDfK)}] with pure **3** against these cell lines. We noted that at these concentrations, blank MWCNT_{c(RGDfK)} was non-cytotoxic (Table 1, entry 5). In all instances, [3·MWCNT_{c(RGDfK)}] was 4-7 fold more cytotoxic than **3** alone, indicating that the MWCNT_{c(RGDfK)} platform was crucial for delivering the payload to the cancer cells. Therefore, we treated Ishikawa cells with **3** and [3·MWCNT_{c(RGDfK)}] for 6 h and quantitated the cellular Pt levels using ICP-MS. Cells treated with [3·MWCNT_{c(RGDfK)}] exhibited ca. 3-fold higher Pt levels compared to those treated with **3** alone (Fig. S6), demonstrating the excellent internalization of hydrophobic **3** by our MWCNT constructs.

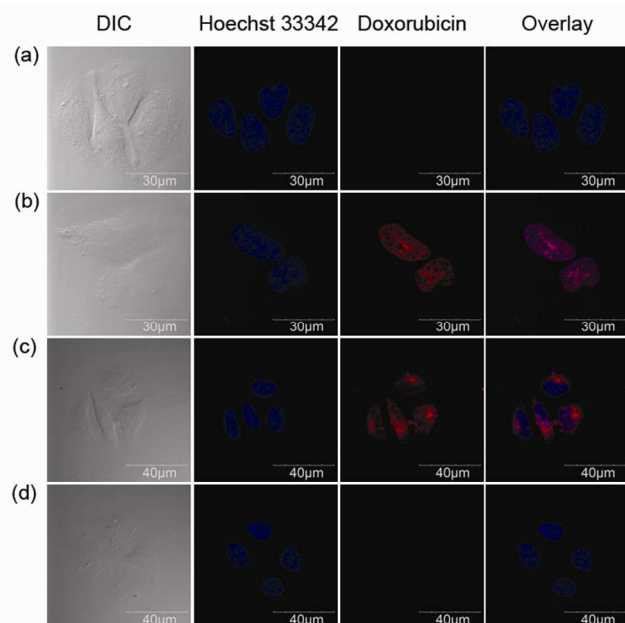


Fig. 5 Merged fluorescence image of Ishikawa cells (a) untreated (control), and exposed to (b) Doxo, (c) [3·MWCNT_{c(RGDfK)}] for 6 h at 37°C, fixed with 4% paraformaldehyde and stained with and Hoechst 33342 (1.3 µg/mL); (d) [3·MWCNT_{c(RGDfK)}] added to fixed/stained untreated cells as background control

In order to show that [3·MWCNT_{c(RGDfK)}] was internalized by cells before releasing the payload, we treated Ishikawa cells with [3·MWCNT_{c(RGDfK)}] for 6 h before fixing and staining with Hoechst 33342 nuclear dye. Although **3** is fluorescent by virtue of its doxo motif, [3·MWCNT_{c(RGDfK)}] does not exhibit fluorescence because it is obscured by its MWCNT carrier. Accordingly, untreated cells that were physically mixed with [3·MWCNT_{c(RGDfK)}] did not exhibit fluorescence within the intracellular or extracellular environment when imaged (Fig. 5d). In contrast, cells that were incubated with [3·MWCNT_{c(RGDfK)}] for 6 h exhibited characteristic fluorescence at $\lambda_{\text{Ex}} = 488 \text{ nm}$; $\lambda_{\text{Em}} = 603 \text{ nm}$ due to the release

of Doxo after internalization and cellular reduction (Fig. 5c). We observed that the released Doxo was distributed throughout the cytoplasm as well as the nucleus. In contrast, cells treated with Doxo were only localized within the nucleus (Fig. 5b). Our hypothesis is that reduction of **3** yielded Doxo that was conjugated to the succinate linker which imparted a negative charge to the conjugated entity. This could delay the translocation of Doxo into the nucleus, leading to an altered distribution profile, and is the subject of ongoing investigations.

Conclusions

With the goal of delivering drug combinations in exact ratiometric proportions against targeted cancers, we developed a nanodelivery platform that released cDDP and a Doxo-derivate when internalized in cancer cells. Therefore, we designed a water-dispersible non-cytotoxic MWCNT-based drug delivery platform that was surface-functionalized with integrin-targeting peptide groups. We also developed a hydrophobic Pt(IV) prodrug, based on the cDDP template and conjugated to Doxo, that could be stably entrapped within the MWCNT interior cavity. We further exploited the intracellular reducing environment to activate Pt(IV) scaffold and release the drug entities. Because the reduced product cDDP and Doxo-derivate were intrinsically hydrophilic, they were efficiently extruded from MWCNT platform. We demonstrated that controlled drug release could be triggered under reducing conditions particularly after the constructs were taken up in cells. These drug-loaded nano-constructs were also highly efficacious *in vitro* especially against endometrial adenocarcinoma cells. This strategy paves the way for the development of combination therapy regimens with precise molecular formulations at the target site for enhanced therapeutic effects.

Acknowledgements

Financial support from Ministry of Education and the National University of Singapore (R143-000-512-112) is gratefully acknowledged.

Notes and references

- (a) G. V. Scagliotti, S. Novello and G. Selvaggi, *Ann. Oncol.*, 1999, **10**, S83; (b) M. P. V. Shekhar, *Curr. Cancer Drug Targets*, 2011, **11**, 613.
- M. M. Gottesman, *Annu. Rev. Med.*, 2002, **53**, 615.
- A. Persidis, *Nat. Biotech.*, 1999, **17**, 94.
- R. Agarwal and S. B. Kaye, *Nat. Rev. Cancer*, 2003, **3**, 820.
- C. M. Hu, S. Aryal and L. Zhang, *Ther. Deliv.*, 2010, **1**, 323.
- (a) C.-M. J. Hu and L. Zhang, *Biochem. Pharmacol.*, 2012, **83**, 1104; (b) M. E. Davis, Z. Chen and D. M. Shin, *Nat. Rev. Drug Discov.*, 2008, **7**, 771.
- T. Lammers, V. Subr, K. Ulbrich, P. Peschke, P. E. Huber, W. E. Hennink and G. Storm, *Biomaterials*, 2009, **30**, 3466.
- (a) B. Rosenberg, L. Van Camp and T. Krigas, *Nature*, 1965, **205**, 698; (b) B. Rosenberg, L. Van Camp, J. E. Trosko and V. H.

- Mansour, *Nature*, 1969, **222**, 385; (c) L. Kelland, *Nat. Rev. Cancer*, 2007, **7**, 573.
- 9 A. Horwich, J. Shipley and R. Huddart, *Lancet*, 2006, **367**, 754.
- 10 (a) H. von der Maase, L. Andersen, L. Crinò, S. Weinknecht and L. Dogliotti, *Ann. Oncol.*, 1999, **10**, 1461; (b) G. Colucci, R. Labianca, F. Di Costanzo, V. Gebbia, G. Carteni, B. Massida, E. Dapretto, L. Manzione, E. Piazza, M. Sannicolò, M. Ciaparrone, L. Cavanna, F. Giuliani, E. Maiello, A. Testa, P. Pederzoli, M. Falconi, C. Gallo, M. Di Maio and F. Perrone, *J. Clin. Oncol.*, 2010, **28**, 1645; (c) H. von der Maase, L. Sengelov, J. T. Roberts, S. Ricci, L. Dogliotti, T. Oliver, M. J. Moore, A. Zimmermann and M. Arning, *J. Clin. Oncol.*, 2005, **23**, 4602.
- 11 G. Giaccone, A. Ardizzoni, A. Kirkpatrick, M. Clerico, T. Sahmoud and N. van Zandwijk, *J. Clin. Oncol.*, 1996, **14**, 814.
- 12 (a) D. Schrijvers, C. Van Herpen, J. Kerger, E. Joosens, C. Van Laer, A. Awada, D. Van den Weyngaert, H. Nguyen, C. Le Boudier, J. A. Castelijns, J. Kaanders, P. De Mulder and J. B. Vermorken, *Ann. Oncol.*, 2004, **15**, 638; (b) F. Keil, E. Selzer, A. Berghold, S. Reinisch, K. S. Kapp, A. De Vries, R. Greil, B. Bachtary, C. Tinchon, W. Anderhuber, M. Burian, A.-K. Kasperek, W. Elsässer, H. Kainz, R. Riedl, M. Kopp and G. Kornek, *Eur. J. Cancer*, 2013, **49**, 352.
- 13 E. R. Jamieson and S. J. Lippard, *Chem. Rev.*, 1999, **99**, 2467.
- 14 D. Wang and S. J. Lippard, *Nat. Rev. Drug Discov.*, 2005, **4**, 307.
- 15 M. A. Fuertes, C. Alonso and J. M. Pérez, *Chem. Rev.*, 2003, **103**, 645.
- 16 (a) M. Bigioni, A. Benzo, C. Irrisuto, G. Lopez, B. Curatella, C. A. Maggi, S. Manzini, A. Crea, S. Caroli, F. Cubadda and M. Binaschi, *Cancer Chemother. Pharmacol.*, 2008, **62**, 621; (b) J. L. Nitiss, *Nat. Rev. Cancer.*, 2009, **9**, 338.
- 17 (a) J. Eder, B. Teicher, S. Holden, L. Senator, K. S. Cathcart and L. Schnipper, *Cancer Chemother. Pharmacol.*, 1990, **26**, 423; (b) F. Ali-Osman, M. S. Berger, S. Rajagopal, A. Spence and R. B. Livingston, *Cancer Res.*, 1993, **53**, 5663; (c) A. Saleem, n. Ibrahim, M. Patel, X.-G. Li, E. Gupta, J. Mendoza, P. Pantazis and E. H. Rubin, *Cancer Res.*, 1997, **57**, 5100.
- 18 M. S. Aapro, F. H. van Wijk, G. Bolis, B. Chevallier, M. E. L. van der Burg, A. Poveda, C. F. de Oliveira, S. Tumolo, V. Scotto di Palumbo, M. Piccart, M. Franchi, F. Zanaboni, A. J. Lacave, R. Fontanelli, G. Favalli, P. Zola, J. P. Guastalla, R. Rosso, C. Marth, M. Nooij, M. Presti, C. Scarabelli, T. A. W. Splinter, E. Ploch, L. V. A. Beex, W. ten Bokkel Huinink, M. Forni, M. Melpignano, P. Blake, P. Kerbrat, C. Mendiola, A. Cervantes, A. Goupil, P. G. Harper, C. Madronal, M. Namer, G. Scarfone, J. E. G. M. Stoot, I. Teodorovic, C. Coens, I. Vergote and J. B. Vermorken, *Ann. Oncol.*, 2003, **14**, 441.
- 19 (a) T. H. Guthrie, Jr., L. J. McElveen, E. S. Porubsky and J. D. Harmon, *Cancer*, 1985, **55**, 1629; (b) O. Lyass, A. Hubert and A. A. Gabizon, *Clin. Cancer Res.*, 2001, **7**, 3040; (c) M. Honda, A. Miura, Y. Izumi, T. Kato, T. Ryotokuji, K. Monma, J. Fujiwara, H. Egashira and T. Nemoto, *Dis. Esophagus*, 2010, **23**, 641; (d) G. F. Fleming, V. L. Brunetto, D. Cella, K. Y. Look, G. C. Reid, A. R. Munkarah, R. Kline, R. A. Burger, A. Goodman and R. T. Burks, *J. Clin. Oncol.*, 2004, **22**, 2159.
- 20 S.-M. Lee, T. V. O'Halloran and S. T. Nguyen, *J. Am. Chem. Soc.*, 2010, **132**, 17130.
- 21 N. Kolishetti, S. Dhar, P. M. Valencia, L. Q. Lin, R. Karnik, S. J. Lippard, R. Langer and O. C. Farokhzad, *Proc. Natl. Acad. Sci. U. S. A.*, 2010, **107**, 17939.
- 22 (a) E. Heister, V. Neves, C. Lamprecht, S. R. P. Silva, H. M. Coley and J. McFadden, *Carbon*, 2012, **50**, 622; (b) Z. Ji, G. Lin, Q. Lu, L. Meng, X. Shen, L. Dong, C. Fu and X. Zhang, *J. Colloid Interface Sci.*, 2012, **365**, 143.
- 23 (a) J. Z. Zhang, P. Bonnitcha, E. Wexselblatt, A. V. Klein, Y. Najajreh, D. Gibson and T. W. Hambley, *Chem. Eur. J.*, 2013, **19**, 1672; (b) V. Pichler, S. M. Valiahd, M. A. Jakupec, V. B. Arion, M. Galanski and B. K. Keppler, *Dalton Trans.*, 2011, **40**, 8187; (c) S. Mukhopadhyay, C. M. Barnes, A. Haskel, S. M. Short, K. R. Barnes and S. J. Lippard, *Bioconjug. Chem.*, 2008, **19**, 39; (d) K. R. Barnes, A. Kutikov and S. J. Lippard, *Chem. Biol.*, 2004, **11**, 557; (e) D. Y. Q. Wong, J. Y. Lau and W. H. Ang, *Dalton Trans.*, 2012, **41**, 6104; (f) L. J. Parker, L. C. Italiano, C. J. Morton, N. C. Hancock, D. B. Ascher, J. B. Aitken, H. H. Harris, P. Campomanes, U. Rothlisberger, A. De Luca, M. Lo Bello, W. H. Ang, P. J. Dyson and M. W. Parker, *Chem. Eur. J.*, 2011, **17**, 7806; (g) W. H. Ang, I. Khalaila, C. S. Allardyce, L. Juillerat-Jeanerret and P. J. Dyson, *J. Am. Chem. Soc.*, 2005, **127**, 1382.
- 24 M. D. Hall, H. R. Mellor, R. Callaghan and T. W. Hambley, *J. Med. Chem.*, 2007, **50**, 3403.
- 25 J. Li, S. Q. Yap, C. F. Chin, Q. Tian, S. L. Yoong, G. Pastorin and W. H. Ang, *Chem. Sci.*, 2012, **3**, 2083.
- 26 C. F. Chin, Q. Tian, M. I. Setyawati, W. Fang, E. S. Q. Tan, D. T. Leong and W. H. Ang, *J. Med. Chem.*, 2012, **55**, 7571.
- 27 W. H. Ang, S. Pilet, R. Scopelliti, F. Bussy, L. Juillerat-Jeanerret and P. J. Dyson, *J. Med. Chem.*, 2005, **48**, 8060.
- 28 T. R. Nayak, P. C. h. i. n. Leow, P.-L. R. a. c. h. e. I. Ee, T. Arockiadoss, S. Ramaprabhu and G. Pastorin, *Curr. Nanosci.*, 2010, **6**, 141.
- 29 M. D. Pierschbacher and E. Ruoslahti, *Nature*, 1984, **309**, 30.
- 30 (a) A. Erdreich-Epstein, H. Shimada, S. Groshen, M. Liu, L. S. Metelitsa, K. S. Kim, M. F. Stins, R. C. Seeger and D. L. Durden, *Cancer Res.*, 2000, **60**, 712; (b) R. Haubner, R. Gratiyas, B. Diefenbach, S. L. Goodman, A. Jonczyk and H. Kessler, *J. Am. Chem. Soc.*, 1996, **118**, 7461.
- 31 E. Sivridis, *Anticancer Res.*, 2001, **21**, 4383.
- 32 R. C. Todd and S. J. Lippard, *Metallomics*, 2009, **1**, 280.
- 33 (a) N. Graf, W. H. Ang, G. Zhu, M. Myint and S. J. Lippard, *Chembiochem*, 2011, **12**, 1115; (b) W. H. Ang, M. Myint and S. J. Lippard, *J. Am. Chem. Soc.*, 2010, **132**, 7429.
- 34 L. A. Zwelling, E. Bales, E. Altschuler and J. Mayes, *Biochem. Pharmacol.*, 1993, **45**, 516.